

Article Processing Dates: Received on 2023-03-28, Reviewed on 2023-05-30, Revised on 2023-06-04, Accepted on 2023-06-06, and Available online on 2023-06-30

Analysis of liquid rocket propellant in nitroglycerin injector reactors

Maryono*, Muhammad Akhlis Rizza

Mechanical Engineering Department, Politeknik Negeri Malang, Malang 57139, Indonesia

*Corresponding author: maryono250375@gmail.com

Abstract

The propulsion of the rocket is due to the thrust resulting from the combustion rate. The propellant energy can be increased by increasing the fuel pressure and temperature of the propellant. Increasing the pressure and temperature of the propellant will increase its combustion rate and the operating conditions of the rocket motor. The most effective liquid propellant used is Nitroglycerin (NG). Nitroglycerin was prepared using the glycerol nitration method with the principle of an injector-based reactor. Therefore, in this research, nitroglycerin was made using the Injector Reactor method with variations in flow rate and injection volume. The results showed that the effect of variations in flow rate and solution volume on the synthesis of nitroglycerin caused a change in solution temperature. Flow rate is closely related to the volume of solution used. The higher the temperature produced, the more heat energy will increase so that the pressure and combustion rate of the propellant increase. The most optimum results use a flow rate of 200 $\mu\text{m/s}$ and a solution volume of 6 ml of glycerin, nitric acid, and sulfuric acid each with a temperature of 37.6°C.

Keywords: Glycerin Nitration, Injector, Nitroglycerin, Reactor, Rocket Liquid Propellant, Temperature

1 Introduction

The need for rockets in military weapons in Indonesia is increasing. The research and development of rockets strengthen technology for the aviation and space sector. Rockets are spacecraft, missiles, or flying vehicles that get a boost through the rocket's reaction to the rapid release of fluid material coming out of the rocket engine. The action of the exhaust in the combustion chamber and the developer nozzle can make the gas flow at hypersonic velocity, giving rise to a large reactive thrust for the rocket. When the rocket is operating, its movement is caused by the thrust that occurs from the combustion reaction of the propellant. The propellant combustion reaction will produce very high temperatures and pressures so that the rocket will move upward [1][2].

The most widely used propellant in combustion systems is liquid [3][4][5]. Liquid propellant shows advantages such as high density, low volatility, low toxicity and corrosivity, high decomposition temperature ($>300^\circ\text{C}$), and strong hydrophobicity [6] [7][8]. However, liquid propellant has drawbacks, namely most liquid propellant depends on hydrazine and its derivatives as bipropellant fuel, which is very toxic, and carries high risks for handling and transportation, difficulties in synthesis, high costs, and incomplete combustion [9] [10] [11] [12]. Incomplete

combustion will reduce the specific impulse of the fuel, and the formation of solid residues can cause erosion of the engine walls by solid product particles, which is a barrier to the practical application of liquid propellant [13][14].

Recently many researchers designing liquid propellants introduce oxygen-rich nitrate ester groups to cations to regulate oxidation-reduction activity, which can improve combustion properties including larger flame and longer duration of burning time. This shows that the increase in oxygen content plays a positive role to achieve the complete combustion of liquid propellant [13][11].

Nitroglycerin (NG) has three nitrate ester groups in one molecule thus giving this compound a very oxygen-rich nature [15][16]. NG is capable of autocatalytic decomposition under certain storage conditions, and its tendency to migrate during propellant processing and storage has been extensively observed and studied [17][18][19]. In addition, NG is a kind of high-performance energetic material, due to the low melting point of NG (287 K), its amount in the propellant must be limited to prevent excessive degradation of grain strength, thereby placing an upper limit on the performance of NG based propellant., the amount in the propellant must be limited to prevent excessive degradation of grain strength, thereby placing an upper limit on the performance of NG-based propellant [9][15]. NG is incorporated in propellant formulations as a strong explosive liquid [20][21][22][23][24].

The formulation for the formation of NG uses a reversible reaction which is formed from the reaction between glycerol and Nitric Acid. The reaction equilibrium must shift to the right so that the product of NG can be formed. Nitroglycerin equilibrium conversion can be achieved by increasing the mole ratio between Glycerol and mixed acids between HNO_3 and H_2SO_4 from 1/2 to 1/7 [25][26]. The process of forming NG uses the glycerol nitration method. Several researchers carried out safe and efficient nitroglycerin manufacturing processes including using a reactor system with the Schmid, Biazzi, and Nitro Injector processes [27][28]. The reactor system using the nitro injector process has an easier process and requires a lower cost. The NG manufacturing process uses an injector to titrate glycerol and the acid product used. A stream of titrating acid is injected into the injector along with a mixture of glycerin and air [28].

The injector system uses the principle of focused hydrodynamics so that it can reduce the width of the flow focus to facilitate fluid mixing. Molecular diffusion facilitates mixing in less than a few microseconds. Microfluid technology in the nitration process has developed rapidly. Micro fluids are more advantageous than macro fluids in terms of performance and cost [29]. Blonski et al., (2011) the results of his research revealed that two aspects affect flow deformation. First, the distribution of the flow width is not uniform. Second, the shape of the flow depends on the degree of curvature of the flow which can change the channel axis so that the flow becomes asymmetric [30]. The dimensions of the focused hydrodynamic microchannel consist of three inlet channels. The microchannel used consists of three input channels, namely glycerol, sulfuric acid, and nitric acid channels. The most homogeneous mixing concentration uses 10 M [31].

Based on the description of the background that has been explained, the design and performance test of an injector-based NG reactor for rocket propellant will be carried out. The injector system used uses the GRBL application. GRBL is software for motion control that can be uploaded to the Arduino library. Basically, GRBL is a hex file that can be uploaded to the Arduino so that the Arduino can read commands in the form of the given code. GRBL will adjust the injector speed according to the specified variation. The performance of the resulting material depends on variations in flow rates of 100 mm/s, 200 mm/s, and 300 mm/s and variations in the volume of solution injected,

respectively flow rates of 2 ml, 4 ml, and 6 ml. Based on the variations in the experiments carried out, the maximum temperature value will be seen. The higher the temperature, the higher the propulsion energy for the resulting rocket.

2 Research Methods

2.1 Materials

The materials used in this study included glycerin (SAP Chemical), sulfuric acid (Merck KGaA), nitric acid (Merck KGaA), and distilled water. The tools used in this research include injectors, Direct Current (DC) motors (Stepping Motor, Model 17HS4401), adapters, thermocouples (TM-902C Digital Thermometer), and reaction tubes (Pyrex).

2.2 Research procedure

The procedure for designing research and testing the performance of an injector-based nitroglycerin reactor using the GRBL Software (controller application consists of three stages, namely the first stage of designing a nitroglycerin reaction device. The second step is to make a solution of nitroglycerin, sulfuric acid, and nitric acid. The third stage of the experiment.

2.2.1 Nitroglycerin reactor design

The design of the nitroglycerin reactor in this study is shown in Fig. 1.

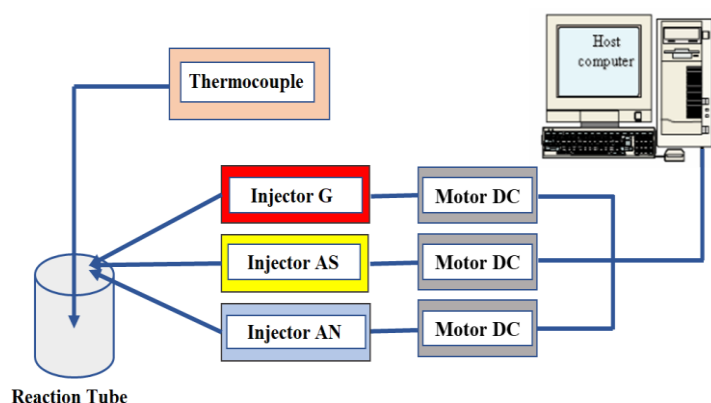


Fig. 1. Nitroglycerin reactor design.

2.2.2 Preparation of solutions of glycerin, sulfuric acid, and nitric acid

The 10 M solution was prepared in three stages. In the first stage, prepared 76.86 ml of glycerin, was then mixed with 100 ml of distilled water. After that, give red coloring. The preparation of the glycerin solution is shown in Fig. 2.

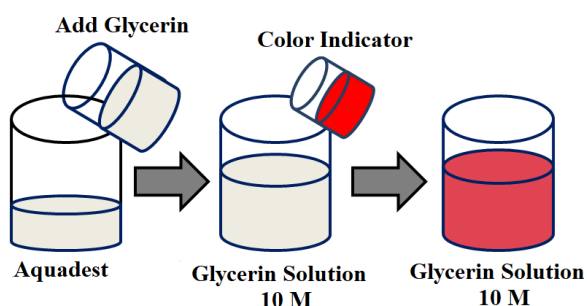


Fig. 2. Preparation of 10 M glycerin solution.

In the second step, prepare 55.56 ml of sulfuric acid, then mix it with 100 ml of distilled water. After that give the yellow coloring. The preparation of the glycerin solution is shown in Fig. 3.

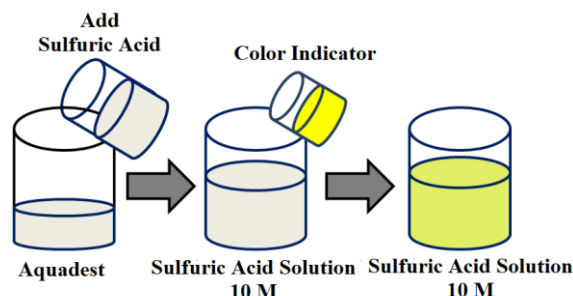


Fig. 3. Preparation of 10 M sulfuric acid solution.

In the third stage, 69.44 ml of nitric acid was prepared, and 100 ml of distilled water was mixed. After that, give it a blue dye. The preparation of the glycerin solution is shown in Fig. 4.

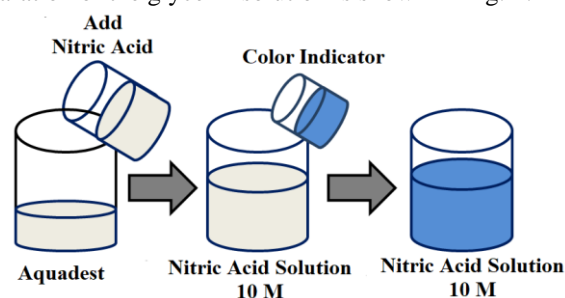


Fig. 4. Preparation of 10 M nitric acid solution.

2.2.3 Experiment

This study uses the help of the GRBL controller application to drive the DC motor so that the injector will issue a solution of nitroglycerin, sulfuric acid, and nitric acid according to the predetermined variations as shown in Fig. 1. The research procedure includes; first of all, is to setting up the equipment according to the research scheme and putting the micro duct with the injector ratio in the position ready for observation. The glycerol, nitric acid, and sulfuric acid solutions used each have a concentration of 10 M.

The solutions are channeled into the test tube using stepper sunshine stepping motor connected to the GRBL application with speeds from 100 mm/s, 200 mm/s, and 300 mm/s. The volume of solution used for each speed is 1 ml, 2 ml, and 3 ml. Then the resulting temperature will be measured in the solution formed using a thermocouple. The data collection formation in this study is shown in Table 1.

Table 1. Formation design of glycerin nitration process data collection.

	Flow Velocity (mm/s)			Reaction Temperature (°C)		
	100	200	300	100	200	300
2 ml	A _{1/200}	B _{1/300}	C _{1/400}			
4 ml	D _{2/200}	E _{2/300}	F _{2/400}			
6 ml	G _{3/200}	H _{3/300}	I _{3/500}			

From data collection, data is obtained in the form of temperature formed in the solution. The results of the temperature measurement data were plotted in graphical form using the Origin Lab program. From the measurement results, then fluid mechanical and chemical analysis was carried out. Analysis was carried out regarding the effect of variations in flow rate and solution volume on the temperature of the resulting solution.

3 Results and Discussion

Nitroglycerin (NG) is a liquid explosive and has the energetic plasticizer properties of polymer-bonded explosives. Its thermal decomposition is closely related to combustion and thermal stability during storage [32]. The autocatalytic decomposition of

NG shows that the first step of the NG decomposition reaction is catalyzed by NO₂ free radicals through the hydrogen abstraction reaction [33]. Nitration is defined as the reaction between an organic compound and a nitrating agent, by adding one or more nitro groups (-NO₂) [34][35]. This reaction is carried out using glycerin and a titrated acid mixture containing nitric acid and sulfuric acid. The chemical reaction for the formation of nitroglycerin in this study is shown in Fig. 5.

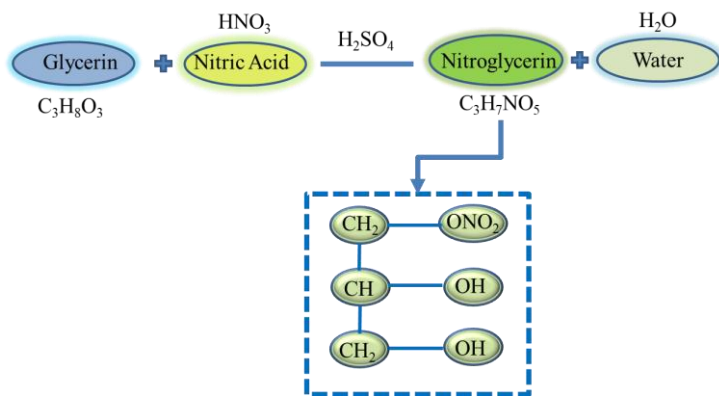


Fig. 5. The chemical reaction for the formation of NG.

Fig. 5 shows the chemical reaction for NG formation by the glycerin nitration method using a microinjector system and GRLB application assistance for microfluidic engineering. Nitration of glycerol, or the production of Nitroglycerin, is an important but very dangerous process that occurs very rapidly and is exothermic. This causes the temperature to rise rapidly which, if not properly controlled, will cause an explosion [36][37]. This high risk of explosion demonstrates the importance of safe and efficient control of the glycerol nitration process. Improving or controlling fluid mixing is often a major design aspect of microfluidic devices [38].

A safe process for nitrating glycerol requires a highly exothermic reaction, so it is important to thoroughly study not only the reaction process but also the method to carry it out [39][40][41]. In addition, the interaction between fluid mechanics and chemical reactions is a very interesting topic because it can affect mass transfer and other transfer phenomena [42][43][44][38]. Microfluidic technology provides a means to overcome some of the most pressing drawbacks of conventional synthesis methods due to the small capillary dimensions and the resulting large surface-to-volume ratio. Through these features, fast and uniform mass transfer, and superior control over the characteristics of the resulting nanomaterials are possible in microfluidic synthesis [45]. Compared to the bulk method, highly stable and uniform monodisperse particles with higher encapsulation efficiency can be obtained by efficiently controlling the geometry of the microfluidic platform and the flow rate of the fluid involved [46].

The working principle of microfluidic devices is based on the movement of fluids in micro-scale channels and special geometric spaces, integrating sample preparation, reaction, separation, and detection [47][48]. The flow type microreactor is shown in Fig. 6.

Regarding the synthesis strategy, there are two main types of microreactors depending on the manipulation of flow patterns, namely, single-phase (continuous flow microfluidics) and multi-phase flow (droplet-based microfluidics) [49][50]. In microfluidic devices, single-phase systems are the most used. The flow pattern has homogeneity characteristics and can control process parameters, such as flow, amount of reagent, reaction time, and temperature [51][52]. The advantages of microfluidic system synthesis are shown in Table 1.

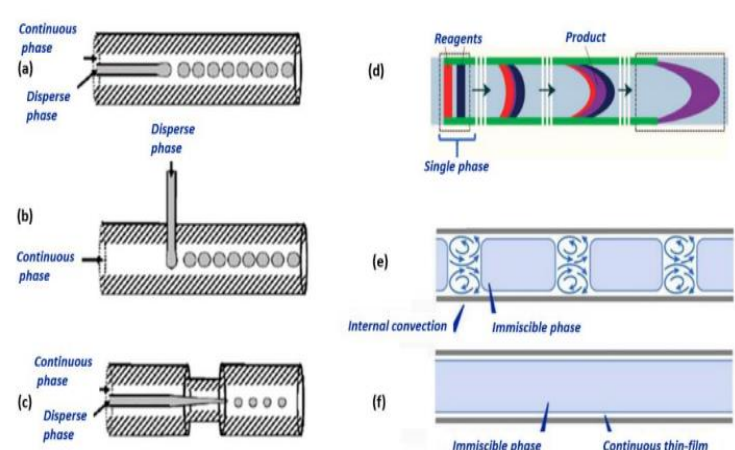


Fig. 6. Common types of microfluidic flow: (a) co-flow, (b) cross-flow, (c) flow-focusing, (d) continuous flow, (e) slug flow, and (f) annular flow [39][40] [41].

Table 1. Advantages of synthesis with a microfluidic system.			
Advantages	Observation	Reference	
High reproducibility	<ul style="list-style-type: none"> Reduce batch-to-batch variation Reproducible composition, streams, and physicochemical properties 	[51][52]	
Well-controlled heat transfer	<ul style="list-style-type: none"> Due to the large surface-to-volume ratio Possibility of rapid heating and cooling of the reaction mixture Temperature homogeneity The need is only a small heat capacity 	[51][52][49][53][54]	
Short reaction time	In the order of minutes	[55][54][56]	
Rapid change of experimental conditions	In microseconds	[58]	
Save costs	<ul style="list-style-type: none"> Energy material and energy inputs are required to reduce synthesis costs Ability of automation reduces labor requirements and labor-related costs 	[51][54][56][57]	
High throughput	Higher percent yield compared to conventional reactors, due to precise control over reaction parameters allowing better selectivity to the desired synthesis product	[51][56][58]	

One way to improve process safety and efficiency of fast exothermic reactions is to reduce the internal volume of the reactor system by using microreactor technology [59][60][61][62]. Due to the flow structure in sub-millimeter dimensions in addition to microreactors, mass, and heat transfer can be greatly intensified compared to conventional batch reactors, and this can offer the possibility to carry out reactions under isothermal conditions, such as nitration, sulphonation, and oxidation [63][64][65]. In addition, the smaller volume of containment microreactors provides high operational safety for handling the synthesis of energetic materials and for investigating their chemical behavior [66][67]. The nitration process in a microreactor has demonstrated the safety characteristics of the microreactor and the possibility to optimize the reaction by studying the effect of the dependent parameters on the reaction rate [63][68][69][70]. The mechanism of increasing the rate of mass transfer and nitration can be controlled in the intrinsic kinetics regime in the microreactor [63][60][70]

The mechanism of nitration of organic compounds using mixed acids $\text{HNO}_3\text{-H}_2\text{SO}_4$ is a well-established process to produce nitrating compounds. The basic mechanism uses H_2SO_4 to catalyze the formation of NO^{2+} from HNO_3 . Thus, the concentration of sulfuric acid in the mixed acid phase plays an important role in the alcohol nitration process because it affects not only the reaction rate but also the product distribution. The strength of sulfuric acid (mass percentage of sulfuric acid in the total mass of sulfuric acid and water) is generally used to determine the type of reaction developed, which permits operation in kinetic or mass transfer control regimes when the remaining parameters are held constant. This model assumes that organic nitration occurs in the aqueous phase close to the interface and is controlled by mass transfer of the organic phase across the liquid-liquid two-phase interface, and the reaction occurs in the mixed acid phase [53].

In this study, variations in the speed of the injector thrust were 100, 200, and 300 $\mu\text{m/s}$, and variations in the volume of glycerin, nitric acid, and sulfuric acid solutions were 2, 4, 6 ml with a solution concentration of 10 M. The research results for making NG using a volume of glycerin solution, 2 ml of nitric acid, and sulfuric acid each with variations in the speed of 100, 200, and 300 $\mu\text{m/s}$ are shown in Fig. 7. The graph of the effect of increasing speed on the temperature in a 2 ml volume of solution is shown in Fig. 8. The duration of the temperature change is shown in Table 2.

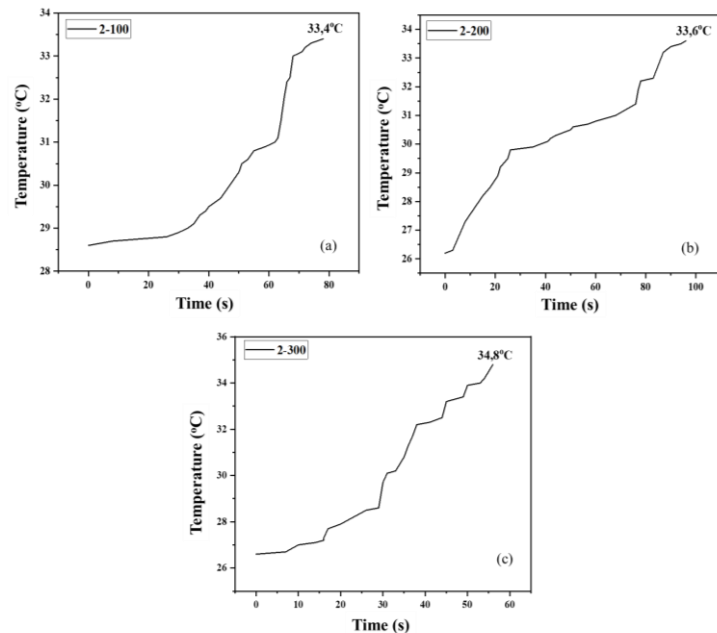


Fig. 7. Effect of NG temperature rate with variations in speed (a) 100, (b) 200, and (c) 300 $\mu\text{m/s}$ with a volume of 2 ml of each solution and a concentration of 10 M.

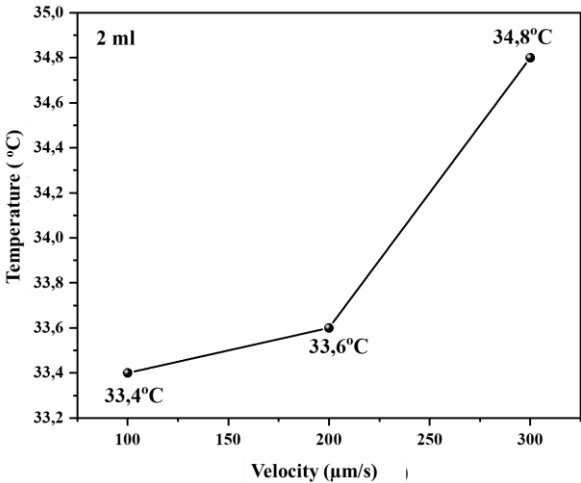


Fig. 8. Graph of the effect of increasing speed on temperature resulting in a volume of 2 ml.

Table 2. The length of the temperature change at speed variations of 100, 200, and 300 with a volume of 2 ml of glycerin, nitric acid, and sulfuric acid solutions.

Speed Variation ($\mu\text{m/s}$)	Long rate of temperature change (s)
100	98
200	108
300	73

Fig. 7, shows a graph of the effect of the NG temperature rate on speed variations of 100, 200, and 300 $\mu\text{m/s}$ using a solution of glycerin, nitric acid, and sulfuric acid each 2 ml with a concentration of 10 M. Table 2, shows that the increase in speed The injector thrust provided from 100 to 200 $\mu\text{m/s}$ causes a long optimum temperature change rate. When the injector thrust speed is increased to 300 $\mu\text{m/s}$, the optimum temperature change rate becomes shorter. The higher the injector speed, the greater the momentum of the liquid coming out of the injector [71]. The faster the temperature change reaches the optimum point, the faster the combustion reaction will result in the NG material. So that in this study the optimum results used an injector thrust speed of 300 $\mu\text{m/s}$ with a volume of 2 ml of glycerin, nitric acid, and sulfuric acid solution. In Fig. 7, the speed variation of 100 $\mu\text{m/s}$ forms an optimum temperature of 33.4°C. The speed variation of 200 $\mu\text{m/s}$ creates an optimum temperature of 33.6°C. The speed variation of 300 $\mu\text{m/s}$ creates an optimum temperature of 34.8°C. Generally, the firing rate increases or decreases as the pressure is increased or decreased. The combustion rate is also affected by the temperature of the propellant if the temperature increases, the combustion rate increases and if the temperature decreases, the combustion rate decreases. The combustion rate also depends on the heating value of the propellant, the higher the heating value, the higher the combustion rate of the propellant [72]. Thus, the optimal temperature is formed at a speed variation of 300 $\mu\text{m/s}$ with a temperature of 34.8°C.

The results of research on making NG using a volume of glycerin, nitric acid, and sulfuric acid solutions of 4 ml each with variations in the speed of 100, 200, and 300 $\mu\text{m/s}$ are shown in Fig. 9. The duration of the temperature change is shown in Table 3. Table 3 shows that increasing the injector thrust speed given from 100 to 300 $\mu\text{m/s}$ causes a difference in the length of the optimum temperature change rate. The increasing the thrust speed of the injector, the faster the resulting optimum temperature change rate. The higher the injector speed, the greater the momentum of the liquid coming out of the injector [71]. The faster

the temperature change reaches the optimum point, the faster the combustion reaction will result in the NG material. So that in this study the optimum results used an injector thrust speed of 300 $\mu\text{m/s}$ with a volume of 4 ml of glycerin, nitric acid, and sulfuric acid solution.

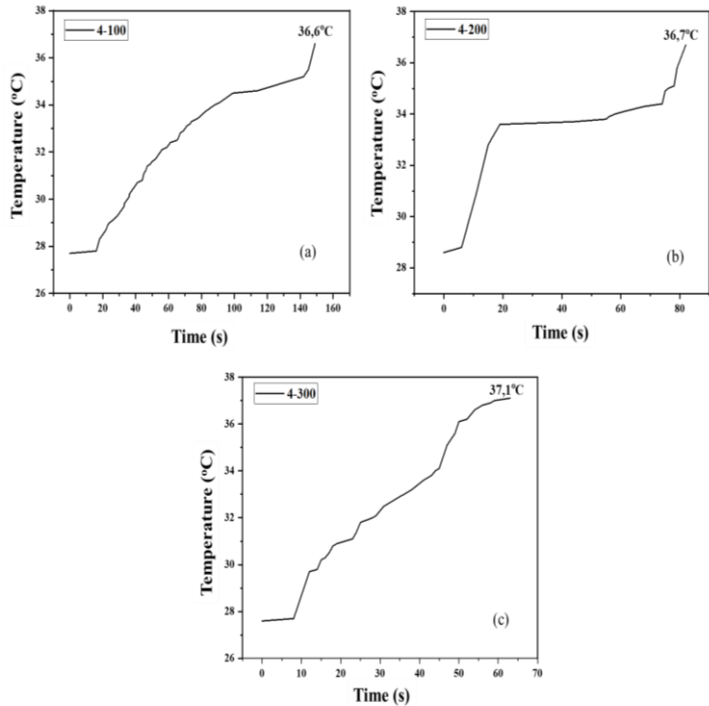


Fig. 9. Effect of NG temperature with variations in speed (a) 100, (b) 200, and (c) 300 $\mu\text{m/s}$ with a volume of 4 ml of each solution and a concentration of 10 M.

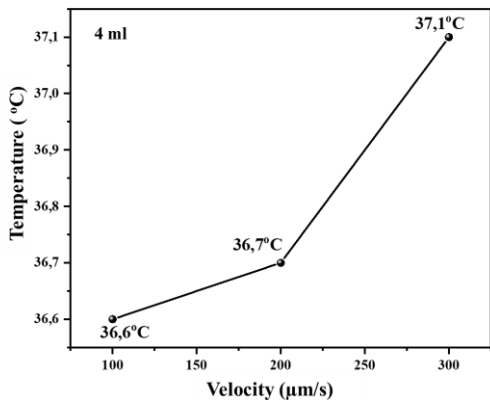


Fig. 10. Graph of the effect of increasing speed on temperature resulting in a volume of 4 ml.

Table 3. The length of the temperature change at speed variations of 100, 200, and 300 with a volume of 4 ml of glycerin, nitric acid, and sulfuric acid solutions.

Speed Variation ($\mu\text{m/s}$)	Long rate of temperature change (s)
100	180
200	98
300	75

Fig. 10 shows a speed variation of 100 $\mu\text{m/s}$, forming an optimum temperature of 36.6°C. The speed variation of 200 $\mu\text{m/s}$ creates an optimum temperature of 36.7°C. The speed variation of 300 $\mu\text{m/s}$ creates an optimum temperature of 37.1°C. Thus, as the speed increases, the resulting temperature change increases. The optimal temperature is formed at a speed variation of 300 $\mu\text{m/s}$ with a temperature of 37.1°C. The rate of combustion increases

when the temperature of the propellant used is higher. The higher the temperature of the propellant, the higher the heat energy produced [72]. The results of research on making NG using a volume of 6 ml of glycerin, nitric acid, and sulfuric acid each with variations in the speed of 100, 200, and 300 $\mu\text{m/s}$ are shown in Fig. 11. The duration of the temperature change is shown in Table 4.

Table 4. The length of the temperature change at speed variations of 100, 200, and 300 with a volume of 6 ml of glycerin, nitric acid, and sulfuric acid solutions.

Speed Variation ($\mu\text{m/s}$)	Long rate of temperature change (s)
100	242
200	119
300	116

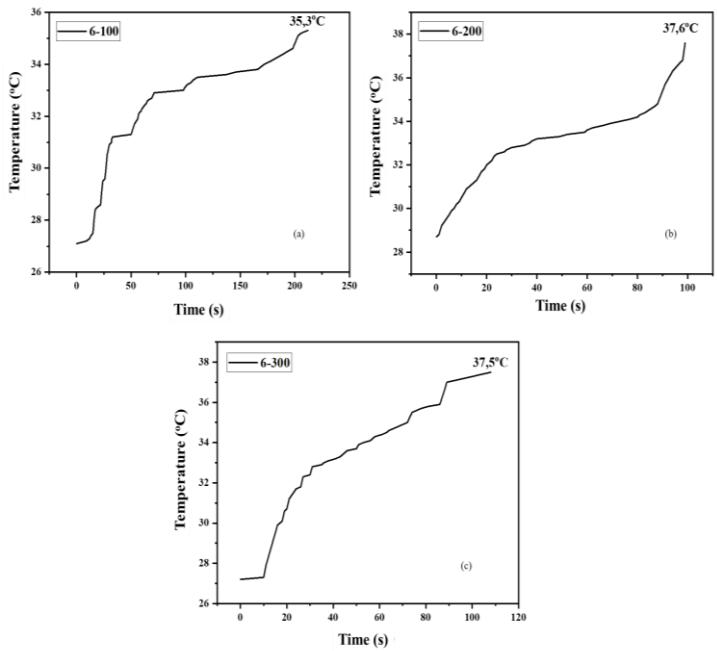


Fig. 11. Effect of NG temperature with variations in speed (a) 100, (b) 200, and (c) 300 $\mu\text{m/s}$ with a volume of 6 ml of each solution and a concentration of 10 M.

Table 4 and Fig. 11, show that increasing the injector thrust speed given from 100 to 300 $\mu\text{m/s}$ causes a difference in the length of the optimum temperature change rate. The higher the injector thrust speed, the faster the resulting optimum temperature change rate. The faster the temperature change reaches the optimum point, the faster the combustion reaction will result in the NG material. So that in this study the optimum results were produced using an injector thrust speed of 200 $\mu\text{m/s}$ with a solution volume of 6 ml of glycerin, nitric acid, and sulfuric acid.

Fig. 12 shows a graph of the effect of the NG temperature rate on speed variations of 100, 200, and 300 $\mu\text{m/s}$ using a solution of glycerin, nitric acid, and sulfuric acid each 6 ml with a concentration of 10 M. At a speed variation of 100 $\mu\text{m/s}$ formed optimum temperature of 35.3°C. The speed variation of 200 $\mu\text{m/s}$ creates an optimum temperature of 37.6°C. The speed variation of 300 $\mu\text{m/s}$ creates an optimum temperature of 37.5°C. Increasing the speed from 100 to 200 causes an increase in the optimum temperature produced $\mu\text{m/s}$. When the boost speed of the injector is increased to 300 $\mu\text{m/s}$ it causes the resulting optimum temperature to decrease. The higher the propellant temperature, the higher the combustion rate and the resulting heat energy [72]. So that in this study the highest optimal temperature was formed

using a variation of the injector thrust speed of 200 $\mu\text{m/s}$ with a temperature of 37.6°C.

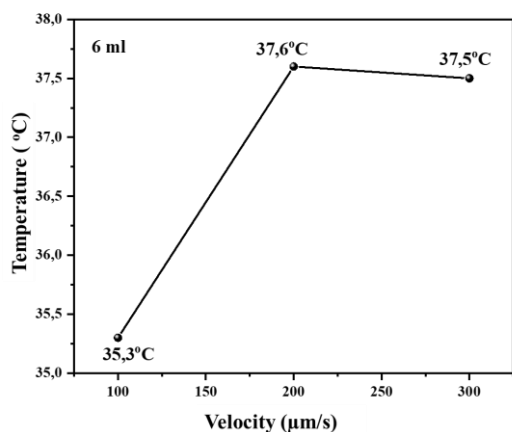


Fig. 12. Graph of the effect of increasing speed on temperature resulting in a volume of 6 ml.

Based on the research that has been done, droplet length is a measure of the volume of droplets produced. Relative displacement is a measurement of the likelihood of droplet interactions in that droplets that are closer together are more likely to interact (perhaps merge) than droplets with a greater relative distance. The measurement of falling velocity is proportional to the velocity of the surrounding fluid, so its value is also a measure of the velocity of the continuous-phase fluid. However, the presence of surfactant can change this measurement because the speed will be affected by chemical injection in the form of Marangoni stress [73][74][75][76][77]. During the dispersion of the solution, the surface tension gradient of the driving force is balanced by the viscous forces in the liquid. Marangoni stress-driven dispersion at the air-liquid interface can be categorized into dispersion on the liquid support used [78][73][79][80][81][74][82][83]. So that if the viscosity of the solution has the same concentration, in this study the addition of the volume of the solution has an important effect on changes in solution temperature. Based on the research analysis results, the graph of the effect of adding the volume of solution on the resulting temperature at an injector thrust speed of 100 $\mu\text{m/s}$ is shown in Fig. 13.

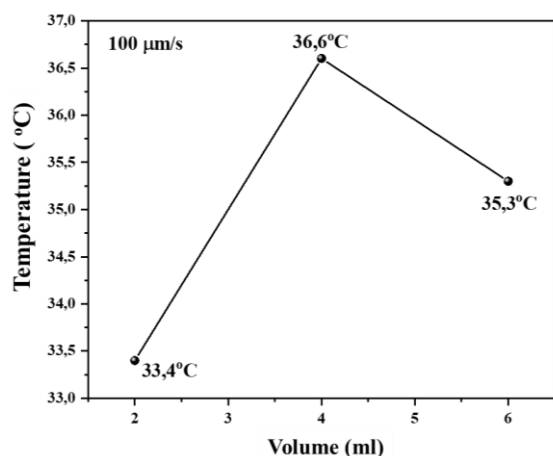


Fig. 13. The effect of adding volume to the resulting temperature at a speed of 100 $\mu\text{m/s}$.

Fig. 13, shows the thrust speed of the injector used is 100 $\mu\text{m/s}$ with variations in the change in solution volume of 2, 4, and 6 ml. Increasing the volume of the solution from 2 to 4 ml resulted in an optimum temperature of 33.4°C and 36.6°C respectively, these

results showed that the resulting optimum temperature was getting higher. When the volume was added to 6 ml it showed an optimum temperature decrease of 35.3°C. So that when using an injector thrust speed of 100 $\mu\text{m/s}$, the volume of a glycerol solution, nitric acid, and sulfuric acid used is 4 ml each. The graph of the effect of increasing the volume on the resulting temperature at the injector thrust speed of 200 $\mu\text{m/s}$ is shown in Fig. 14.

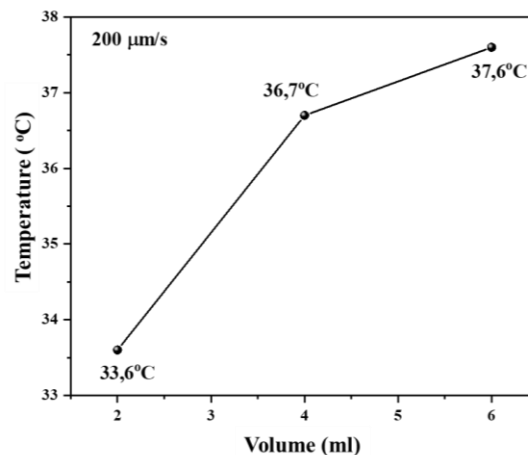


Fig. 14. Graph of the effect of increasing the volume on the resulting temperature at a speed of 200 $\mu\text{m/s}$.

Fig. 14, shows the thrust speed of the injector used is 200 $\mu\text{m/s}$ with variations in the change in solution volume of 2, 4, and 6 ml. Variations in the volume of the 2 ml solution produce an optimum temperature of 33.6°C, variations in the volume of the 4 ml solution produce an optimum temperature of 36.7°C, and variations in the volume of the 6 ml solution produce an optimum temperature of 37.6°C. As the volume of solution used increases, the resulting optimum temperature increases. So that when using an injector thrust speed of 200 $\mu\text{m/s}$, the volume of a glycerol solution, nitric acid, and sulfuric acid used is 6 ml each. The graph of the effect of increasing volume on temperature resulted in an injector boost speed of 300 $\mu\text{m/s}$ is shown in Fig. 15. Fig. 15, shows that the injector thrust speed used was 300 $\mu\text{m/s}$ with variations in solution volume changes of 2, 4, and 6 ml. Variations in the volume of the 2 ml solution produce an optimum temperature of 34.8°C, variations in the volume of the 4 ml solution produce an optimum temperature of 37.1°C, and variations in the volume of the 6 ml solution produce an optimum temperature of 37.5°C. As the volume of solution used increases, the resulting optimum temperature increases. So that when using an injector thrust speed of 300 $\mu\text{m/s}$, the volume of a glycerol solution, nitric acid, and sulfuric acid used is 6 ml each.

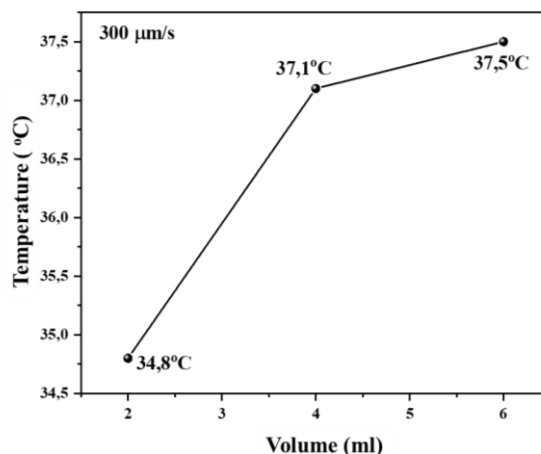


Fig. 15. Graph of the effect of increasing the volume on the resulting temperature at a speed of 300 $\mu\text{m/s}$.

The combustion rate of the rocket propellant depends on several factors related to the ignition rate, pressure, and initial temperature of the propellant [84]. The energy of the propellant can be increased by increasing the pressure and temperature of the propellant. Increasing the temperature of the propellant will increase the heat energy produced so that the pressure, the combustion rate, and the operation of the rocket motor increase [84] [85]. Based on the results of the research analysis, the optimum temperature of 37.6°C was found at a variation of the injector thrust speed of 200 µm/s with variations in the volume of glycerin, nitric acid, and sulfuric acid each of 6 ml.

The results of this research apply the Maxwell-Boltzman principle which provides an understanding of kinetic chemical processes involving biomolecular collisions. Molecular collisions are one of the most important events that occur in Nature, affecting almost every aspect of our lives. Molecular collisions have a direct influence on a variety of phenomena including thermal conduction (heat transfer), diffusion (mass transfer), viscous effect (momentum transfer), friction (heat dissipation), and chemical reactions [86][87][88][89][90][91][92][93][94]. The rate of a chemical reaction can be empirically related to the reaction temperature using the following general expression (Eq. 1) [95].

$$k(T)=bT^m \dots\dots\dots 1$$

where k is the chemical reaction rate, T is the reaction temperature, and b and m are the characteristic parameters of each chemical reaction [95].

4. Conclusion

The effect of variations in flow rate and solution volume on the synthesis of nitroglycerin causes a change in solution temperature. Flow rate is closely related to the volume of solution used. The most optimal results use a flow rate of 200 µm/s and a solution volume of 6 ml of glycerin, nitric acid, and sulfuric acid, each with a temperature of 37.6°C.

Reference

- [1] J. Thongsri, K. Srathonghuam, and A. Boonpan, "Gas Flow and Ablation of 122 mm Supersonic Rocket Nozzle Investigated by Conjugate Heat Transfer Analysis," *Processes*, vol. 10, no. 9, 2022, doi: 10.3390/pr10091823.
- [2] C. Griego, N. Yilmaz, and A. Atmanli, "Analysis of aluminum particle combustion in a downward burning solid rocket propellant," *Fuel*, vol. 237, no. October 2018, pp. 405–412, 2019, doi: 10.1016/j.fuel.2018.10.016.
- [3] V. K. Bhosale, S. Karnik, and P. S. Kulkarni, "Ignition study of amine borane/cyanoborane based green hypergolic fuels," *Combust. Flame*, vol. 210, pp. 1–8, 2019, doi: 10.1016/j.combustflame.2019.08.015.
- [4] S. Soller *et al.*, "Design and Testing of Liquid Propellant Injectors for Additive Manufacturing," *Eucass*, no. Eucass, 2017.
- [5] M. Son, K. Radhakrishnan, J. Koo, O. C. Kwon, and H. D. Kim, "Design procedure of a movable pintle injector for liquid rocket engines," *J. Propuls. Power*, vol. 33, no. 4, pp. 858–869, 2017, doi: 10.2514/1.B36301.
- [6] W. Zhang, X. Qi, S. Huang, J. Li, and Q. Zhang, "Super-base-derived hypergolic ionic fuels with remarkably improved thermal stability," *J. Mater. Chem. A*, vol. 3, no. 41, pp. 20664–20672, 2015, doi: 10.1039/c5ta05559h.
- [7] T. Liu *et al.*, "Exploiting hydrophobic borohydride-rich ionic liquids as faster-igniting rocket fuels," *Chem. Commun.*, vol. 52, no. 10, pp. 2031–2034, 2016, doi: 10.1039/c5cc09737a.
- [8] A. E. S. Nosseir, A. Cervone, and A. Pasini, "Review of

- state-of-the-art green monopropellants: For propulsion systems analysts and designers," *Aerospace*, vol. 8, no. 1, pp. 1–21, 2021, doi: 10.3390/aerospace8010020.
- [9] Q. Zhang and J. M. Shreeve, "Energetic Ionic Liquids as Explosives and Propellant Fuels: A New Journey of Ionic Liquid Chemistry," 2014, doi: 10.1021/cr500364t.
- [10] S. Schneider, T. Hawkins, M. Rosander, G. Vaghjiani, S. Chambreau, and G. Drake, "Ionic Liquids as Hypergolic Fuels," no. 11, pp. 2871–2872, 2008.
- [11] Z. Wang *et al.*, "From heart drug to propellant fuels: Designing nitroglycerin-ionic liquid composite as green high-energy hypergolic fluids," *Combust. Flame*, vol. 233, p. 111597, 2021, doi: 10.1016/j.combustflame.2021.111597.
- [12] P. D. McCrary *et al.*, "Hypergolic ionic liquids to mill, suspend, and ignite boron nanoparticles," *Chem. Commun.*, vol. 48, no. 36, pp. 4311–4313, 2012, doi: 10.1039/c2cc30957b.
- [13] Y. Wang, S. Huang, W. Zhang, T. Liu, X. Qi, and Q. Zhang, "Nitrate-Functionalized Task-Specific Ionic Liquids as Attractive Hypergolic Rocket Fuels," *Chem. - A Eur. J.*, vol. 23, no. 51, pp. 12502–12509, 2017, doi: 10.1002/chem.201701804.
- [14] A. J. Mundahl *et al.*, "Characterization of a novel ionic liquid monopropellant for multi-mode propulsion," *53rd AIAA/SAE/ASEE Jt. Propuls. Conf. 2017*, no. July, pp. 1–20, 2017, doi: 10.2514/6.2017-4756.
- [15] Y. Zhou, H. Gao, and J. M. Shreeve, "Dinitromethyl groups enliven energetic salts," *Energ. Mater. Front.*, vol. 1, no. 1, pp. 2–15, 2020, doi: 10.1016/j.enmf.2020.04.001.
- [16] Z. Yu *et al.*, "Simulation for the migration of nitrate ester plasticizers in different liners contacting with propellant by molecular dynamics," *J. Energ. Mater.*, vol. 39, no. 1, pp. 74–84, 2021, doi: 10.1080/07370652.2020.1756987.
- [17] F. Jutz, J.-M. Andanson, and A. Baiker, "ChemInform Abstract: Ionic Liquids and Dense Carbon Dioxide: A Beneficial Biphasic System for Catalysis," *ChemInform*, vol. 42, no. 21, p. no-no, 2011, doi: 10.1002/chin.201121239.
- [18] B. Ni and A. D. Headley, "Ionic-Liquid-Supported (ILS) catalysts for asymmetric organic synthesis," *Chem. - A Eur. J.*, vol. 16, no. 15, pp. 4426–4436, 2010, doi: 10.1002/chem.200902747.
- [19] Q. Zhang, S. Zhang, and Y. Deng, "Recent advances in ionic liquid catalysis," *Green Chem.*, vol. 13, no. 10, pp. 2619–2637, 2011, doi: 10.1039/c1gc15334j.
- [20] H. J. Maag and G. Klingenberg, "Gun propulsion concepts. Part II: Solid and liquid propellants," *Propellants, Explos. Pyrotech.*, vol. 21, no. 1, pp. 1–7, 1996, doi: 10.1002/prep.19960210102.
- [21] Z. P. Huang, H. Y. Nie, Y. Y. Zhang, L. M. Tan, H. L. Yin, and X. G. Ma, "Migration kinetics and mechanisms of plasticizers, stabilizers at interfaces of NEPE propellant/HTPB liner/EDPM insulation," *J. Hazard. Mater.*, vol. 229–230, pp. 251–257, 2012, doi: 10.1016/j.jhazmat.2012.05.103.
- [22] D. Venkatesan, M. Srinivasan, K. A. Reddy, and V. V. Pendse, "The migration of plasticizer in solid propellant grains," *Polym. Int.*, vol. 32, no. 4, pp. 395–399, 1993, doi: 10.1002/pi.4990320410.
- [23] D. A. Reese, L. J. Groven, and S. F. Son, "Formulation and characterization of a new nitroglycerin-free double base propellant," *Propellants, Explos. Pyrotech.*, vol. 39, no. 2, pp. 205–210, 2014, doi: 10.1002/prep.201300105.
- [24] R. J. Buszek *et al.*, "Structures and Binding Energies of Nitrate Plasticizers DEGDN, TEGDN, and Nitroglycerine," *Propellants, Explos. Pyrotech.*, vol. 43,

- no. 2, pp. 115–121, 2018, doi: 10.1002/prep.201700203.
- [25] E. Astuti and A. Prasetya, "Optimum Operating Condition Of Glycerol Nitration," *ARNP J. Eng. Appl. Sci.*, vol. 11, no. 8, pp. 5203–5208, 2016.
- [26] S. Gayathri and S. Reshmi, "Nitrate Functionalized Polymers for High Energy Propellants and Explosives: Recent Advances," *Polym. Adv. Technol.*, vol. 28, no. 12, pp. 1539–1550, 2017, doi: 10.1002/pat.4039.
- [27] T. Urbanski, "Structure of Cellulose—Nitric Acid Knecht Compounds. I. Spectroscopic Examination," *Org. Chem.*, vol. XIII, no. 6, pp. 377–383, 1965, [Online]. Available: http://bcpw.bg.pw.edu.pl/Content/3747/bulletin_de_lacademie_polonaise_des_sciences_1965_nr6_s377.pdf.
- [28] R. K. Weaver, "The Changing World of Think Tanks," *PS Polit. Sci. Polit.*, vol. 22, no. 3, p. 563, 1989, doi: 10.2307/419623.
- [29] G. M. Walker, H. C. Zeringue, and D. J. Beebe, "Microenvironment design considerations for cellular scale studies," *Lab Chip*, vol. 4, no. 2, pp. 91–97, 2004, doi: 10.1039/b311214d.
- [30] W. Blonski, A. M. Buchner, and G. R. Lichtenstein, "Inflammatory bowel disease therapy: Current state-of-the-art," *Curr. Opin. Gastroenterol.*, vol. 27, no. 4, pp. 346–357, 2011, doi: 10.1097/MOG.0b013e328347aef3.
- [31] S. Susilo, Gumono, and B. Irawan, "The Effect of Concentration Reactant to Mixing Nitroglycerin Using Microchannel Hydrodynamics Focusing," *J. Southwest Jiaotong Univ.*, vol. 17, no. 3, 2020.
- [32] T. Zeng, R. Yang, J. Li, W. Tang, and D. Li, "Thermal Decomposition Mechanism of Nitroglycerin by ReaxFF Reactive Molecular Dynamics Simulations," *Combust. Sci. Technol.*, vol. 193, no. 3, pp. 470–484, 2021, doi: 10.1080/00102202.2019.1661999.
- [33] L. Matteo, "Numerical Simulation of Nitrous Oxide Catalytic Decomposition," 2017.
- [34] I. Kazakov *et al.*, "Study of Nitration Equilibrium in The Glycerin-Aqueous Nitric Acid System," *Plenum Publ. Corp.*, no. 8, pp. 1729–1734, 1990.
- [35] Erna Astuti, Supranto, Rochmadi, and A. Prasetya, "A Thermodynamic Study of Parameters That Affect the Nitration of Glycerol with Nitric Acid," *J. Chem. Mol. Eng.*, vol. 9, no. 8, pp. 1010–1013, 2015.
- [36] W. Baraboo, "Applied Innovative Technologies for Characterization of Nitrocellulose and Nitroglycerine Contaminated Buildings and Soils," U.S., 2008.
- [37] K. Lu and P. Lin, "Study on the stability of nitroglycerine spent acid," *Process Saf. Environ. Prot.*, vol. 7, no. 87, pp. 87–93, 2009, doi: 10.1016/j.psep.2008.08.004.
- [38] R. Wulandari, I. N. G. Wardana, and S. Wahyudi, "Reactive Mixing Behavior of the Nitration of Glycerin in a Stirred Vessel at Various Perturbation," *Appl. Mech. Mater.*, vol. 493, pp. 221–226, 2014, doi: 10.4028/www.scientific.net/AMM.493.221.
- [39] S. Guo, Q. Wang, J. Sun, X. Liao, and Z. Wang, "Study on the influence of moisture content on thermal stability of propellant," *J. Hazard. Mater.*, vol. 168, pp. 536–541, 2009, doi: 10.1016/j.jhazmat.2009.02.073.
- [40] K. Katoh, M. Nakahama, S. Kawaguchi, M. Arai, and Y. Wada, "The effects of conventional stabilizers and phenolic antioxidants on the thermal stability of nitroglycerine," *Sci. Tech. Energ. Mater.*, vol. 71, pp. 17–23, 2010.
- [41] A. Rifai and E. . Finalis, "Towards The Independence of The Propellant Industry for Munitions and Rocket," *J. Mater. dan Proses Manufaktur*, vol. 6, no. 2, pp. 54–61, 2022.
- [42] H. Aref, "Order in chaos," *Macmillan Magazine*, vol. 401, no. October, pp. 2–4, 1999.
- [43] F. . Moon, *Chaotic and Fractal Dynamics: An Introduction for Applied Scientists and Engineers*. 1996.
- [44] P. K. Pandey, A. K. Sharma, and U. Gupta, "Blood Brain Barrier: An overview on Strategies in Drug Delivery , Realistic In Vitro Modelling and In Vivo Live Tracking," *J. Tissue Barriers*, vol. 8370, no. December, 2015, doi: 10.1080/21688370.2015.1129476.
- [45] D. Liu, S. Cito, Y. Zhang, C. F. Wang, T. M. Sikanen, and H. A. Santos, "A versatile and robust microfluidic platform toward high throughput synthesis of homogeneous nanoparticles with tunable properties," *Adv. Mater.*, vol. 27, no. 14, pp. 2298–2304, 2015, doi: 10.1002/adma.201405408.
- [46] S. Damiani, U. B. Kompella, S. A. Damiani, and R. Kodzius, "Microfluidic devices for drug delivery systems and drug screening," *Genes (Basel)*, vol. 9, no. 2, 2018, doi: 10.3390/genes9020103.
- [47] S. Hamdallah *et al.*, "Microfluidics for pharmaceutical nanoparticle fabrication: the truth and the myth," *Int. J. Pharm.*, vol. 584, pp. 12–26, 2020.
- [48] D. Zhang, H. Bi, B. Liu, and L. Qiao, "Detection of Pathogenic Microorganisms by Microfluidics Based Analytical Methods," *Anal. Chem.*, vol. 90, no. 9, pp. 5512–5520, 2018, doi: 10.1021/acs.analchem.8b00399.
- [49] V. S. Cabeza, "High and Efficient Production of Nanomaterials by Microfluidic Reactor Approaches," *Adv. Microfluid. - New Appl. Biol. Energy, Mater. Sci.*, 2016, doi: 10.5772/64347.
- [50] B. Yu, R. J. Lee, and L. J. Lee, "Microfluidic Methods for Production of Liposomes," *Methods Enzymol.*, vol. 465, no. C, pp. 129–141, 2009, doi: 10.1016/S0076-6879(09)65007-2.
- [51] P. Shrimal, G. Jadeja, and S. Patel, "A review on novel methodologies for drug nanoparticle preparation: Microfluidic approach," *Chem. Eng. Res. Des.*, vol. 153, pp. 728–756, 2020, doi: 10.1016/j.cherd.2019.11.031.
- [52] J. Ma, S. M. Y. Lee, C. Yi, and C. W. Li, "Controllable synthesis of functional nanoparticles by microfluidic platforms for biomedical applications-a review," *Lab Chip*, vol. 17, no. 2, pp. 209–226, 2017, doi: 10.1039/C6LC01049K.
- [53] S. Jiani, Z. Yuchao, C. Guangwen, and Y. Quan, "Investigation of Nitration Processes of iso -Octanol with Mixed Acid in," *Chinese J. Chem. Eng.*, vol. 17, no. 3, pp. 412–418, 2009.
- [54] P. Sengupta, K. Khanra, A. R. Chowdhury, and P. Datta, *Lab-on-a-chip sensing devices for biomedical applications*. Elsevier Ltd, 2019.
- [55] C. X. Zhao, L. He, S. Z. Qiao, and A. P. J. Middelberg, "Nanoparticle synthesis in microreactors," *Chem. Eng. Sci.*, vol. 66, no. 7, pp. 1463–1479, 2011, doi: 10.1016/j.ces.2010.08.039.
- [56] A. Singh, C. K. Malek, and S. K. Kulkarni, "Development in microreactor technology for nanoparticle synthesis," *Int. J. Nanosci.*, vol. 9, no. 1–2, pp. 93–112, 2010, doi: 10.1142/S0219581X10006557.
- [57] Y. Hu *et al.*, "Facile High Throughput Wet-Chemical Synthesis Approach Using a Microfluidic-Based Composition and Temperature Controlling Platform," *Front. Chem.*, vol. 8, no. November, pp. 1–14, 2020, doi: 10.3389/fchem.2020.579828.
- [58] Y. Song, J. Hormes, and C. S. S. R. Kumar, "Microfluidic synthesis of nanomaterials," *Small*, vol. 4, no. 6, pp. 698–711, 2008, doi: 10.1002/sml.200701029.
- [59] S. J. Haswell, R. J. Middleton, B. O. Sullivan, and V. Skelton, "The application of micro reactors to synthetic

- chemistry,” *Chem. Commun.*, pp. 391–398, 2001, doi: 10.1039/b008496o.
- [60] G. Dummann, U. Quittmann, L. Gröschel, D. W. Agar, O. Wörz, and K. Morgenschweis, “The capillary-microreactor: a new reactor concept for the intensification of heat and mass transfer in liquid – liquid reactions,” *Catal. Today*, vol. 80, pp. 433–439, 2003, doi: 10.1016/S0920-5861(03)00056-7.
- [61] G. Panke, T. Schwalbe, W. Stirner, S. Taghavi-Moghadam, and G. Wille, “A Practical Approach of Continuous Processing to High Energetic Nitration Reactions in Microreactors,” *Adv. online Publ.*, vol. 3, pp. 2827–2830, 2003, doi: 10.1055/s-2003-42491.
- [62] G. Chen, Q. Yuan, H. Li, and S. Li, “CO selective oxidation in a microchannel reactor for PEM fuel cell,” *Chem. Eng. J.*, vol. 101, no. 1–3, pp. 101–106, 2004, doi: 10.1016/j.cej.2004.01.020.
- [63] J. R. Burns and C. Ramshaw, “Chemical Engineering Communications A Microreactor for the Nitration of Benzene and Toluene,” *Chem. Eng. Commun.*, vol. 189, no. 12, pp. 1611–1628, 2002.
- [64] A. Muller, V. Cominos, V. Hessel, B. Horn, J. Sch, and A. Ziogas, “Fluidic bus system for chemical process engineering in the laboratory and for small-scale production,” *Chem. Eng. J.*, vol. 107, pp. 205–214, 2005, doi: 10.1016/j.cej.2004.12.030.
- [65] B. A. A. Woezik and K. R. Westerterp, “The nitric acid oxidation of 2-octanol. A model reaction for multiple heterogeneous liquid-liquid reactions,” *Chem. Eng. Process. Process Intensif.*, vol. 39, no. 6, pp. 521–537, 2000, doi: 10.1016/S0255-2701(00)00099-4.
- [66] K. Jähnisch, V. Hessel, H. Löwe, and M. Baerns, *Chemistry in Microstructured Reactors*, vol. 43, no. 4, 2004.
- [67] M. Brivio, W. Verboom, and D. N. Reinhoudt, “Miniaturized continuous flow reaction vessels: Influence on chemical reactions Miniaturized continuous flow reaction vessels: influence on chemical reactions,” *R. Soc. Chem.*, vol. 6, no. June 2014, pp. 329–344, 2006, doi: 10.1039/b510856j.
- [68] L. Ducry and D. M. Roberge, “Controlled Autocatalytic Nitration of Phenol in a Microreactor,” *Chem. Int.*, vol. 44, pp. 7972–7975, 2005, doi: 10.1002/anie.200502387.
- [69] L. Henke and H. Winterbauer, “A Modular Micro Reactor for Mixed Acid Nitration,” *Chem. Eng. Technol.*, vol. 28, 2005, doi: 10.1002/ceat.200500096.
- [70] R. Halder, A. Lawal, and R. Damavarapu, “Nitration of toluene in a microreactor,” *Catal. Today*, vol. 125, pp. 74–80, 2007, doi: 10.1016/j.cattod.2007.04.002.
- [71] J. Manin, M. Bardi, L. M. Pickett, and R. Payri, “Boundary condition and fuel composition effects on injection processes of high-pressure sprays at the microscopic level,” *Int. J. Multiph. Flow*, vol. 83, pp. 267–278, 2016, doi: 10.1016/j.ijmultiphaseflow.2015.12.001.
- [72] V. V. Kulkarni, A. R. Kulkarni, P. A. Phawade, and J. P. Agrawal, “A study on the effect of additives on temperature sensitivity in composite propellants,” *Propellants, Explos. Pyrotech.*, vol. 26, no. 3, pp. 125–129, 2001, doi: 10.1002/1521-4087(200106)26:3<125::AID-PREP125>3.0.CO;2-8.
- [73] B. N. D. Dipietro, C. Huh, and R. G. Cox, “The hydrodynamics of the spreading of one liquid on the surface of another,” *J. Fluid Mech.*, vol. 84, pp. 529–549, 1978.
- [74] O. . Jensen, “The spreading of insoluble surfactant at the free surface of a deep fluid layer,” *J. Fluid Mech.*, vol. 293, pp. 349–378, 1995.
- [75] J. . Scott, “Flow beneath a stagnant film on water: the Reynolds ridge,” *J. Fluid Mech.*, vol. 116, pp. 283–296, 1982.
- [76] B. J. F. Harper, “The leading edge of an oil slick, soap film, or bubble stagnant cap in Stokes flow,” *J. Fluid Mech.*, vol. 237, pp. 23–32, 1992.
- [77] J. L. Bull and J. B. Grotberg, “Surfactant spreading on thin viscous films: film thickness evolution and periodic wall stretch,” *Exp. Fluids*, vol. 34, pp. 1–15, 2003, doi: 10.1007/s00348-002-0447-2.
- [78] D. . Hoult, “Oil Spreading On the Sea,” *Annu. Rev. Fluid Mech.*, vol. 341, no. 1, 1972.
- [79] M. Foda and C. Rg, “The spreading of thin liquid films on a water-air interface,” *J. Fluid Mech.*, vol. 101, pp. 33–51, 1980.
- [80] A. D. Dussaud and S. M. Troian, “Dynamics of spontaneous spreading with evaporation on a deep fluid layer,” *Am. Inst. Phys.*, vol. 10, pp. 23–38, 1998.
- [81] D. . Camp and J. . Berg, “The spreading of oil on water in the surface-tension regime,” *J. Fluid Mech.*, vol. 184, pp. 445–462, 2012, doi: 10.1017/S0022112087002969.
- [82] D. . Suci, O. Smigelschi, and E. Ruckenstein, “The Spreading of Liquids on Liquids,” *J. Colloid Interface Sci.*, vol. 88, no. 4, pp. 520–528, 1970.
- [83] C. Huh, M. Inoue, and S. . Mason, “Uni . Directional Spreading of One Liquid on T h e Surface of Another,” *J. Chem. Eng.*, vol. 53, pp. 367–371, 1975.
- [84] X. G. Wu, Q. L. Yan, X. Guo, X. F. Qi, X. J. Li, and K. Q. Wang, “Combustion efficiency and pyrochemical properties of micron-sized metal particles as the components of modified double-base propellant,” *Acta Astronaut.*, vol. 68, no. 7–8, pp. 1098–1112, 2011, doi: 10.1016/j.actaastro.2010.09.028.
- [85] H. Yaman, V. Çelik, and E. Degirmenci, “Experimental investigation of the factors affecting the burning rate of solid rocket propellants,” *Fuel*, vol. 115, pp. 794–803, 2014, doi: 10.1016/j.fuel.2013.05.033.
- [86] H. Hernandez and F. Research, “Clausius’ molecular sphere of action in crowded systems: Non-ideal gas behavior,” *ForsChem Res. Reports*, vol. 2, no. 11, pp. 1–16, 2017, doi: 10.13140/RG.2.2.36384.07681.
- [87] H. Hernandez and J. Aguirre, “Clausius’ Entropy change during molecular collisions,” *ForsChem Res. Reports*, vol. 045, no. 17, 2017, doi: 10.13140/RG.2.2.33917.97764.
- [88] H. Hernandez, “Collision Energy between Maxwell-Boltzmann Molecules: An Alternative Derivation of Arrhenius Equation,” *ForsChem Res. Reports*, vol. 4, no. 13, pp. 1–27, 2019, doi: 10.13140/RG.2.2.21596.33926.
- [89] H. Hernandez, “Probability Distributions of Molecular Kinetic Energy and Molecular Temperature,” *ForsChem Res. Reports*, vol. 4, no. 12, pp. 1–12, 2019, doi: 10.13140/RG.2.2.32880.00005.
- [90] H. Hernandez, “Molecular Free Path Statistical Distribution of Multicomponent Systems,” *ForsChem Res. Reports*, vol. 6, no. May, 2017, doi: 10.13140/RG.2.2.15605.58088.
- [91] H. Hernandez and F. Research, “Multicomponent Molecular Diffusion: A Mathematical Framework,” *ForsChem Res. Reports*, vol. 2, no. 9, pp. 1–22, 2017, doi: 10.13140/RG.2.2.14828.46724.
- [92] H. Hernandez, “Multicomponent Molecular Collision Kinetics: Rigorous Collision Time Distribution,” *ForsChem Res. Reports*, no. June, 2017, doi: 10.13140/RG.2.2.26218.31689.
- [93] H. Hernandez, “Multicomponent Molecular Collision Kinetics: Collision Rate and the Collision Frequency Paradox,” *ForsChem Res. Reports*, no. June, 2017, doi:

10.13140/RG.2.2.32983.27048.

- [94] H. Hernandez, "Clausius' sphere of action for different intermolecular potentials," *ForsChem Res. Reports*, vol. 2, no. 10, pp. 1–27, 2017, doi: 10.13140/RG.2.2.25246.23363.
- [95] S. R. Logan, "The origin and status of the arrhenius equation," *J. Chem. Educ.*, vol. 59, no. 4, pp. 279–281, 1982, doi: 10.1021/ed059p279.